Geochemical Journal, Vol. 47, pp. 423 to 435, 2013

Isotope and chemical compositions of thermal fluids at Tekman Geothermal Area (Eastern Turkey)

GALIP YUCE[1]* and LUTFI TASKIRAN[2]

[1]Department of Geological Engineering, Faculty of Engineering and Architecture, Eskisehir Osmangazi University, Meselik, Eskisehir, Turkey
[2]Geothermal Survey Division, General Directorate of Mineral Research and Exploration, Ankara, Turkey

(*Received September 12, 2012; Accepted May 10, 2013*)

The aim of this study was to understand geochemistry of thermal fluids circulating in the basin at the southwest of Tekman (Erzurum, Turkey) Geothermal Province in Eastern Anatolia as well as to estimate reservoir temperature and its heat source by assessment of helium and carbon isotopic compositions of liquid and gas samples.

Deep thermal and cold shallow groundwaters are NaCl type (Cerme and Ilipinar springs) and Ca–Mg–HCO_3 type, respectively. The discharge temperatures of thermal waters vary between 29 and 57°C. The reservoir temperatures were estimated by solute silica and cation geothermometers vary from 80 to 110°C. CO_2 is the dominant gas in geothermal fluids with variable amounts of nitrogen, helium and CH_4. The isotopic ratios of helium that range from 1.03 to 1.54Ra_c show a range crustal to magmatic-type values. The isotopic composition of carbon (CO_2) obtained from the bubbling and dissolved gases shows the variation from –0.2 to 3.4‰ vs. PDB. The mantle derived fluids interact at shallower levels with circulating meteoric waters and originate geothermal systems from which equilibration temperatures were estimated up to 192°C by gas geothermometers.

Keywords: geothermal, hydrogeochemistry, isotope, geothermometers, Tekman

INTRODUCTION

Turkey is considered as the seventh richest country in the world regarding geothermal potential (Balat, 2006), since it has more than thousands of thermal and mineral water springs (Canik and Baskan, 1983; Mutlu and Gulec, 1998; Battocletti, 1999; Mertoglu *et al*., 2003; Dagistan *et al*., 2010; Serpen *et al*., 2010). The geothermal fields in Turkey are mainly distributed along the active faults and young volcanic area (Arpat and Saroglu, 1975; Eyidogan, 1988; Balderer, 1997; Yılmaz, 1997; Bozkurt, 2001). High-temperature geothermal sources are mostly discovered in the western part of Turkey. Therefore, many studies have been carried out to investigate chemical and isotopic composition of geothermal waters in Western Turkey (Simsek, 1982; Ercan *et al*., 1985, 1997; Gulec, 1988; Demange *et al*., 1989; Conrad *et al*., 1995; Mützenberg, 1997; Imbach, 1997; Simsek, 1997; Gokgoz, 1998; Ozgur *et al*., 1998; Ozler, 2000; Gurer *et al*., 2001; Gemici and Filiz, 2001; Tarcan, 2002; Vengosh and Helvacı, 2002; Vengosh *et al*., 2002; Tarcan and Gemici, 2003; Ongay, 2004). Eastern Turkey, associated with active faults and volcanic activity, has also a remarkable geothermal potential. However, the geothermal potential in Eastern Turkey has been investigated less in detail (Demirtasli and Pisoni, 1965; Saroglu, 1986; Can *et al*., 1987; Olmez and Güner, 1989; Tarhan, 1991a, b; Tarhan, 1997). Some geothermal studies were also carried out by General Directorate of Mineral Research and Exploration of Turkey (MTA) along with a geological/geophysical prospective study by Taskiran (2006). However, geochemistry of thermal fluids and estimation of reservoir temperature were not examined previously. Thus, the present study aims filling this gap. For this purpose, fieldwork and laboratory analyses were performed. Several water samples were collected from the springs in the study area. *In-situ* measurements were realized to measure the physical and chemical parameters of the water samples. Major and minor ions, environmental isotopes of thermal and cold waters in the area were analyzed. All analytical results and field observations were examined to better understand the geothermal potential of the Tekman Geothermal Area (TGA).

The gas isotopes results show that gas-water interaction (GWI) and variable mixing of mantle-derived and crustal fluids lead to a wide range of geochemical features of the discharged fluids. Conformingly, existence of carbonatic and metamorphic rocks, huge volume of

*Corresponding author (e-mail: galipyuce@gmail.com)

travertine deposits, and old volcanites are good evidences for the different origin of the circulating fluids and different fluid-rock interactions in the study area.

In the light of obtained results from the previous (Taskiran, 2006) and this study, MTA drilled a well in 550 m depth at Cerme nearby the study area. The cap and reservoir rocks proposed by the present study were justified through the lithologies encountered along the well. The bottom temperature of the well is 71°C, consistent with the estimations from geothermometric calculations.

Geological and Hydrogeological Settings

The study area is 400 km^2, located between Tekman town (100 km away from the Erzurum city center) and Bingol city. The annual average air temperature and precipitation are 12.1°C and 817.7 mm/a, respectively. The topography is mostly of sharp relief and cliffs. The alluvial material is deposited on NE-SW direction following the river course.

The geological information related to the study area was acquired from Tarhan (1991b). The geological map is given in Fig. 2.

The oldest rocks in the area are serpentinized dunite and harzburgite, which is the member of the Hinis metaophiolites. The oldest units are overlained by Tertiary volcanic rocks, limestone, and clastic sedimentary units with a tectonic contact. The Tertiary units mainly consist of reddish clastics (conglomerate, sandstone, mudstone), limestone, fine sedimentary units and volcanic rocks (lava and pyroclastic). The sequences of Tertiary units are Kozlu formation, Mollakulacdere formation and Adilcevaz formation from bottom to top that are vertically and horizontally transitional to each other. Middle–Late Miocene aged Kohkale Tepe Lava and Middle–Late Pliocene aged Yolustu formation unconformably overlie oldest formations. Quaternary aged travertine and alluvium are the youngest units, which crop out along the surface flow and cover all oldest units in the area.

The major faults in the study area are NE–SW and NW–SE oriented strike slip faults, parallel to the North and East Anatolian Fault Zones in the southwest of the study area. This strike slip fault system causes to form the extensional fissures where thermal waters emerge to the surface along these fissures, which with the deposition of yellowish-brownish color lisvenite due to thermal water circulation.

The study area is located in the intersection of the EAFZ and NAFZ active faults (Fig. 1). They intersect near Karliova village with an acute angle of 50–60 degree. Nevertheless, the triple junction of East and North Fault Zones in Karliova extend and diverge to the East. The eruption of the Bingol volcano started in Middle–Late Miocene near this intersection of faults (triple junction). The distribution of magmatic products of Miocene and Quaternary Volcanism (after Cetin *et al*., 2003) is shown in Fig. 1. The Bingol Mountain was an active volcanic center as a semi-caldera until Pliocene (2.6–3.1 Ma) (Hurbert-Ferrari *et al*., 2009).

The NE–SW oriented faults and fractures in the area lead to secondary porosity and permeability in the limestone unit of Adilcevaz formation, which is the main thermal aquifer in the area.

Quaternary alluvium and travertine are the aquifers for cold groundwaters. Unaltered and low porous rocks of Miocene volcanism are the cap rocks. The magma chamber of the Bingol Mountain, which was active for the last several years, (Keskin, 2007) was evaluated as the main heat source of the geothermal system in the study area.

The discharge temperatures of thermal waters vary between 29–57°C. However, the cooling process in some thermal waters can be seen due to mixing with cold waters in the southwestern part. The oldest unit (serpentinized dunite and harzburgite) has a very low intrinsic permeability. However, from the hydrogeological point of view, it can be considered as a semipermeable unit due to long-term circulation of thermal water in this unit. The unaltered volcanics (Mivsk) can be considered as the caprocks due to having low permeability. Oligocene formation (Mollakulacdere), Pliocene basalt and andesites are semipermeable due to joints found in their altered zones. Eocene-aged Kozlu formation and Quaternary units are other essential aquifers since they have high permeabilities.

Material and Methods

The fourteen water samples collected for water chemistry and free/dissolved gas composition were taken from twelve thermal and two cold springs at the discharge temperatures from 11.2 to 54.8°C. Water temperature, pH, and electrical conductivity (EC) were measured *in situ* by YSI-556 model multi-parameter handheld instrument with an accuracy of ±0.15°C, ±1 S/cm, and ±0.2, temperature, pH and EC, respectively. All water samples were filtered by 0.45 μcm- and stabilized by ultrapure HNO_3 to avoid any constitution of compounds. The cation-anion balance in $meql^{-1}$ is less than ±5%. Tritium was measured by counting β decay events in the liquid scintillation counting (LSC) method (ISO, 1989) after electrolytic enrichment and error limit was ±1 Tritium Units. The samples prepared in the equilibrium method for oxygen-18 and deuterium measurements were analyzed by the Isotope Ratio Mass Spectrometer (IRMS). Precision limits of δD and δ^{18}O were ±0.5 and ±0.3, respectively. All stable isotope data were annotated in the standard delta notation relative to SMOW.

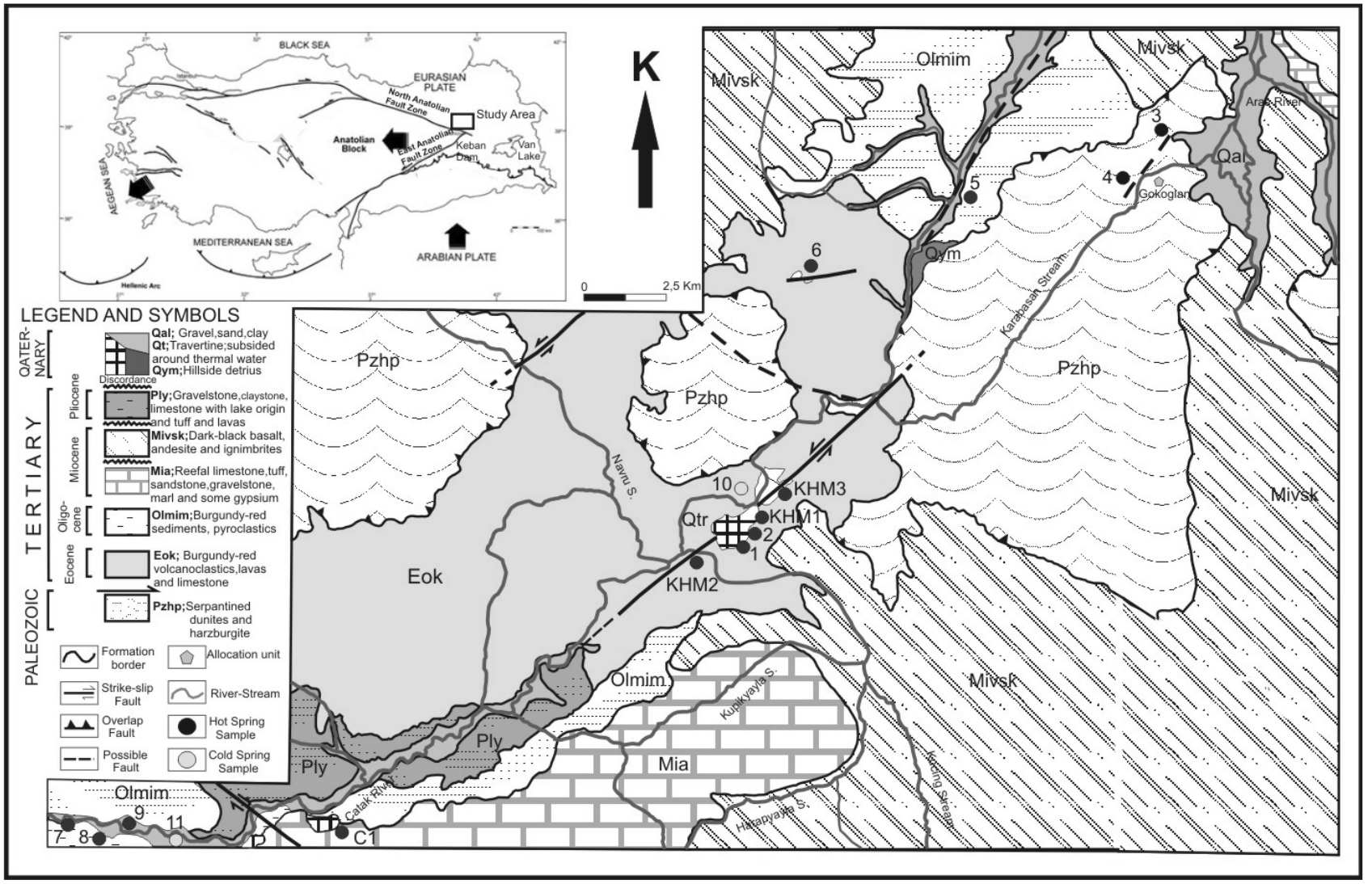

Fig. 1. The geological map of the study area (modified from Tarhan, 1997).

Table 1. Chemical composition of dissolved (D) and bubbling (B) gases of the Tekman geothermal area (modified after Italiano et al., 2013)

Updated samples	Location name	Type	Date	*R/Ra*	He/Ne	[He] corr	[Ne] corr	R/Ra_c	Error	%Atm	%Rad
C1	Catak–Karliova	B	2011.5.27	1.49	25.5	49.3	16.515	1.54	0.018	1.2	73.3
C1	Catak–Karliova	D	2011.5.27	1.17	1.05	2.23E-04	2.12E-04	1.23	0.0237	30.3	54.8
KHM1	Karliova–Hamzan–Catak	D	2011.5.26	1.02	1.49	2.26E-04	1.52E-04	1.03	0.0217	21.3	64.7
KHM2	Karliova–Hamzan–Catak	B	2011.5.27	1.07	29.11	67.2	2.308	1.07	0.013	1.1	80.7
KHM3	Karliova–Hamzan–Catak	D	2011.5.27	1.02	0.52	1.13E-04	2.20E-04	1.03	0.0161	61.1	31.9

Updated samples	%Mag	Rra corr	^{3}He	CO_2	He	O_2	N_2	CH_4	$CO_2/^3$He	δ^{13}C	CO_2 (vol%)	ΔHe/Ne
C1	25.5	1.50	1.0E-04	24.1	5.10E-02	2.68	64.38	8.30E-02	2.00E+08	0.2	24.30	80.2
C1	15.0	1.36	3.6E-10	66.4	3.00E-04	0.3	8.9	1.67E-03	1.83E+11	0.59	90.70	3.7
KHM1	14.0	1.11	3.2E-10	267.1	8.00E-05	1.13	1.57	5.45E-05	8.57E+11	3.4	98.00	5.2
KHM2	18.2	1.07	1.0E-04	83	8.10E-03	0.04	16.27	2.90E-01	6.70E+09	6.7	81.20	91.5
KHM3	7.0	1.48	1.6E-10	296.9	3.50E-05	1.1	1.97	2.18E-03	2.01E+12	—	97.7	1.8

All analytical results were examined by Schoeller, Piper, mixing, ion distribution, and saturation graphics. The software Aqua, 2005 (Rockware, Version 1.1) was used to constrain hydrochemical properties of thermal and cold waters.

All of the gas samples were collected taking care to avoid even tiny bubbles to prevent atmospheric contamination (details in Italiano *et al*., 2009, 2013). The dissolved gases were obtained from water samples stored into 240 ml glass bottles and sealed in the field by rubber septa using special pliers. The bubbling gases were collected using a stainless-steel inverse funnel connected to a three ways valve. The valve was connected to a syringe and to a two-ways pyrex bottle with vacuum stop-cocks at both ends. The syringe sucked the gas collected by the funnel and through the valve; the gas was pushed inside the sampling bottle. The bottle was flushed with a gas amount ten times larger than its volume, and then the sample was stored in.

The chemical composition of He, H_2, O_2, N_2, CO, CH_4 and CO_2 was performed using a Perkin Elmer Clarus 500 gas chromatograph equipped with a double detector (TCD-FID; detection limits 1 ppm/vol), with argon as carrier gas. The bubbling gases were analyzed by direct injection in the gas-chromatograph, while the dissolved gas analyses were carried out on the gas phase extracted after the attainment of the equilibrium (at constant temperature) between the water sample and a known volume of host, high purity gas (argon), injected inside the sampling.

The isotopic composition of helium and carbon were determined by mass spectrometry. Helium isotopes analyses of both bubbling and dissolved gases (on gas fractions extracted following the same procedure as for the gas-chromatography and using nitrogen as host gas) were carried out after accurate samples purification following already proposed procedures (e.g., Italiano *et al*., 2009). The uncertainties in the range of low-^{3}He (radiogenic) samples are within ±1%.

The water samples for dissolved gas analyses were also used for the determination of the carbon isotopic ratio of the total dissolved inorganic carbon (TDIC). The method for $\delta^{13}C_{TDIC}$ determination is based on the chemical and physical stripping of CO_2. The stripped gas, as well as the bubbling CO_2, are purified by means standard procedures (Favara *et al*., 2002), then the carbon isotopic composition and was measured using a Finnigan Delta Plus mass spectrometer and the results expressed in ‰ vs. VPDB standard. The standard deviation of $^{13}C/^{12}C$ ratio is ±0.2‰.

Results and Discussion

Table 1 lists the analytical results of the gas-chromatographic analyses. The composition of the bubbling and dissolved gases are reported as vol% and cm^3 STP/L of water, respectively.

It is believed that the detected oxygen in samples is sourced from the atmosphere and since any deep-originated gas is considered oxygen free. The gas analytical results were re-calculated by removing the atmospheric contribution (using analytical oxygen content versus its theoretical amount in ASW and in the air).

By taking into account the total amount of dissolved gases (cm^3/l at 20°C), we re-calculated the relative abundances of every single gas species and normalized to 100%, which, allow a comparison of the analytical results of both dissolved and bubbling gases. The converted gas analyses (*Cvt*) are shown in columns 9–13 of Table 1.

The measured helium isotopic ratios (reported as *R/Ra* where *R* = measured isotopic ratio and *Ra* = atmospheric $^3He/^4He = 1.39 \times 10^{-6}$) was corrected for the ef-

Table 2. The major-minor ion concentrations and environmental isotope analyses results of the springs in the study area

Water type	$Ca–HCO_3$ type thermal waters						Na–Cl type thermal waters			Mg–Ca HCO_3 type cold waters		Na–Cl type thermal water	$Ca–HCO_3$ type thermal waters	
Sample location	Kigihamzan	Kigihamzan	Gokoglan	Gokoglan	Meman	Yigitler	Cerme	Cerme	Ilipinar	Kigihamzan	Cerme	Cl	KHM1	KHM3
Sample ID	1	2	3	4	5	6	7	8	9	10	11	12*	13*	14*
Analysis date	12/08/2005	12/08/2005	12/08/2005	12/08/2005	12/08/2005	12/08/2005	12/08/2005	12/08/2005	12/08/2005	12/08/2005	12/08/2005	27/05/2011	27/05/2011	27/05/2011
Temperature (°C)	56.9	56.3	35	34	53	51.6	34.9	34.4	29	11.4	11.2	29.7	54.8	41.1
pH	6.8	6.48	6.7	6.37	6.70	6.46	7.2	6.75	6.8	8.17	7.87	6.35	5.95	6.21
EC (μmho/cm)	1235	1315	1808	1850	1407	1515	19630	19570	21100	431	580	24360	2082	725
Total hardness (Ao)	27.1	17.89	49.8	47.17	41	37.8	200	184.4		11.06	10.55	415	52.5	46.2
K^+ (mg/l)	11.5	10.2	14	17	9	11	50	47	180	18	20	38.2	12.9	10.1
Na^+ (mg/l)	70	64	78	74.5	38.5	40	3250	3112	3158	39	45	3902	78.9	58
NH_4^+(mg/l)	2.48	2.55	1.24	Yok	3.1	N/A	3.70	N/A	<0.1	N/A	N/A	N/A	N/A	N/A
Ca^{2+} (mg/l)	111	100	194	176	194	190	1119	1160	1154	20	75	1328	123.2	114.2
Mg^{2+}(mg/l)	50	47.7	98	98	60	55	190	97	2.3	36	3	202.1	52.1	42.4
B (Total)	1.5	1.1	0.5	0.6	0.40	0.37	4	3.89	3.5	0.8	0.9	1.39	1.24	0.89
Cl^- (mg/l)	77	70	74	63	35	40	6257	6000	6500	15	16	392.3	64.3	49.7
Cl/B	51	64	148	105	88	108	1564	1542	1857	19	18	282	52	56
HCO_3^- (mg/l)	556	600	1136	1196	912	942	574	671	429	305	364	341.6	634.4	597.8
CO_3^- (mg/l)	<10	<10	<10	<10	<10	<10	<10	<10	<10	0.45	<10	<10	<10	<10
SO_4^{2-} (mg/l)	60.5	54.9	83	80	75.30	77.68	1969	1913	1790	18	20	109.4	33.2	31.7
NO_2^- (mg/l)	N/A	N/A	<0.1	<0.1	<0.1	<0.1	1	1	<0.1	N/A	<0.1	<0.1	<0.1	<0.1
NaCl (mg/l)	N/A	0.07	N/A	0.09	N/A	0.08	N/A	1.12	N/A	0.02	0.03	N/A	N/A	N/A
Flow (l/s)	3	3.5	4.5	3	5.5	2.7	4	4.5	1.8	2	2.5	~10	3.5	2
Fe (Total)	1	0.89	0.5	0.4	1.80	1.91	4.20	5.11	0.5	0.2	0.40	0.48	0.21	0.03
Li^+ (mg/l)	0.20	0.13	0.12	0.9	<0,1	<0,1	0.23	0.25	0.05	0.04	0.01	0	0	0.22
Mn (Total)	0.07	0.02	0.04	0.04	0.18	0.13	0.10	0.15	<0.01	0.01	<0.01	0.1	0.06	0.03
Pb^{2+} (mg/l)	0.09	0.01	0.04	0.03	0.05	0.06	0.18	0.13	<0.01	0.01	<0.01	<0.01	<0.01	<0.01
Zn^{2+} (mg/l)	<0.03	<0.03	<0.03	<0.03	<0.03	<0.03	<0.03	<0.03	<0.03	<0.03	<0.03	<0.03	<0.03	<0.03
Cd^{2+}(mg/l)	<0.03	<0.03	<0.03	<0.03	<0.03	<0.03	<0.03	<0.03	<0.03	<0.03	<0.03	<0.03	<0.03	<0.03
Cr (mg/l)	<0.03	<0.03	<0.03	<0.03	<0.03	<0.03	0.06	0.08	<0.03	<0.03	<0.03	<0.03	<0.03	<0.03
Ni^{2+} (mg/l)	0.09	0.05	0.08	0.05	0.04	0.04	0.14	0.11	0.03	<0.03	<0.03	0.006	0.05	0.014
Co (mg/l)	<0.03	<0.03	<0.03	<0.03	<0.03	<0.03	0.05	0.04	<0.03	<0.03	<0.03	<0.03	<0.03	<0.03
SiO_2 (mg/l)	64	55	58	56	47	45	32	30	8.6	23	21	N/A	N/A	N/A
Cu (mg/l)	<0.03	<0.03	<0.03	<0.03	<0.03	<0.03	0.04	0.04	<0.03	<0.03	<0.03	<0.03	<0.03	<0.03
$\delta^{18}O$	−12.12	N/A	−12.11	N/A	−12.14	−11.69	−12.18	−12.15	−11.38	−11.62	−11.79	−11.8	−12.14	−11.68
δ^2H	−75.09	N/A	−74.54	N/A	−71.8	−73.63	−71.1	−74.21	−68.03	−73.65	−75.1	−77	−75	−67
Tritium (^3H) (TU)	4.4	N/A	3.75	N/A	2.55	7.05	2.1	2.25	6.7	8.3	13.61	N/A	N/A	N/A
D_{excess}	21.87	N/A	22.34	N/A	25.32	19.89	23.34	23.00	23.01	19.31	19.22	17.4	22.12	26.4

**A. Sasmaz, O. Okan (Firat University, Elazig) personal communication.*

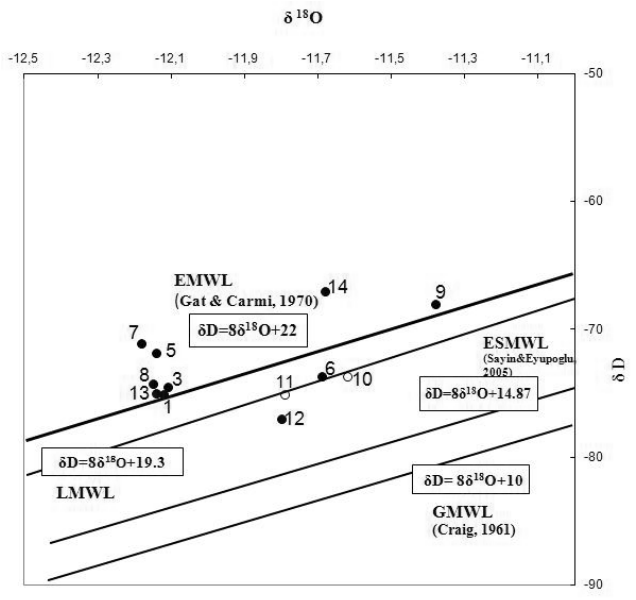

Fig. 2. The isotopic composition of thermal and cold waters plotted on the $\delta^{18}O$ vs. deuterium diagram (GMWL, Global Meteoric Water Line; EMWL, Eastern Meteoric Water Line; LMWL, Local Meteoric Water Line; ESMWL, Erzurum-Senyurt Meteoric Water Line).

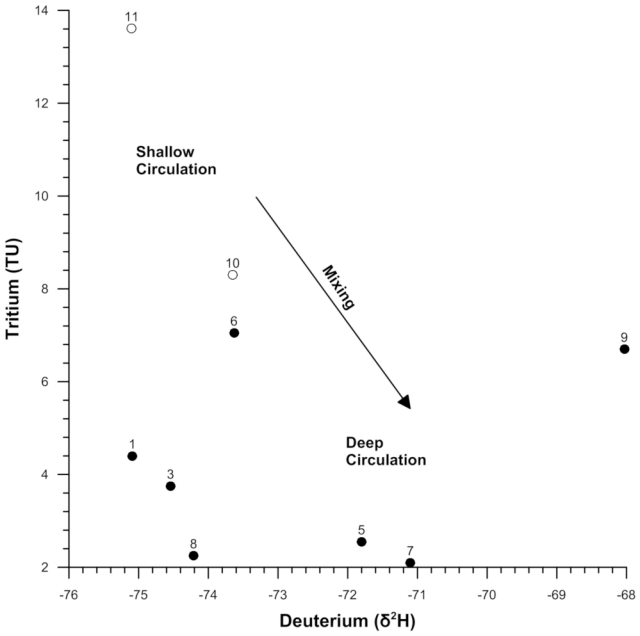

Fig. 3. The δD–Tritium correlation of water samples in the study area.

fects of atmospheric contamination (R/Ra_c values in Table 1) using the air-normalized He/Ne ratio and assuming that all the neon is of atmospheric origin. For dissolved gases, the air-normalized He/Ne ratio was calculated taking into consideration the ratio of their solubility coefficients (Bunsen coefficient "β", Weiss, 1971). Table 1 lists the isotopic composition of helium and carbon as well as the $^4He/^{20}Ne$ ratios. The $^3He/^4He$ ratios (R) have been normalized to the atmosphere ($^3He/^4He = 1.39 \times 10^{-6} = Ra$) and corrected for the effects of atmospheric contamination (R/Ra_C) using $(R/Ra_c) = \{(R/Ra)X–1\}/\{X–1\}$ where X is the air and the ASW He/Ne ratio (Hilton *et al*., 1998) respectively for bubbling and dissolved gases. Carbon isotopic ratios of TDIC and CO_2 express in δ‰ versus the PDB international standard.

Cold and thermal waters

The major-minor ions and environmental isotope results of the springs in the study area are given in Table 2.

The surfacial temperatures of the thermal waters in the study area vary between 29 and 57°C. Twelve samples from the thermal springs and two samples from the cold springs (10 and 11) were collected. Based on the classification, in terms of dominant cation and anion of water samples, three different groundwater facies were recognized (Table 2): I) Kigihamzan, Gokoglan, Meman and Yigitler thermal waters (No. 1, 2, 3, 4, 5, 6, 13 and 14) are Ca–HCO_3 facies; II) Cerme and Ilipinar thermal waters (7, 8, 9 and 12) are Na–Cl facies; III) Kigihamzan and Cerme cold waters (10 and 11) are Mg–Ca HCO_3 facies. The similar chloride/boron ratios (Table 2) are also compatible with above classification. Mg content of Ilipinar thermal spring (No. 9) is rather low. The reason of this low Mg content can be explained by absorption of magnesium in high temperature leveled geothermal systems and absorption of secondary minerals by illite, montmorillonite and especially chlorite (Ongay, 2004). Relatively high silica content in Kigihamzan and Gokoglan thermal waters of group I (1, 2, 4, and 5) are in a good agreement with the higher temperature. Thermal waters of group II show deep circulation.

$\delta^{18}O–\delta D$ compositions

$\delta^{18}O–\delta D$ compositions of waters are given in Table 2. Most waters plot above the Eastern Mediterranean Meteoric Water Line (EMWL) (Fig. 2). The δD and $\delta^{18}O$ of thermal and cold waters are far above the Global Meteoric Water Line (GMWL) and the Erzurum-Senyurt Meteorological Observation Station (ESMWL) (Sayın and Eyuboglu, 2005). This shift is probably due to the precipitation in the region that is affected by evaporation occurring from Keban Dam reservoir and Van Lake (M. Sayın, 2006, personal communication). The occurrence of the lukewarm-low humid air masses with strong kinetic evaporation (i.e., the origination of vapor under low

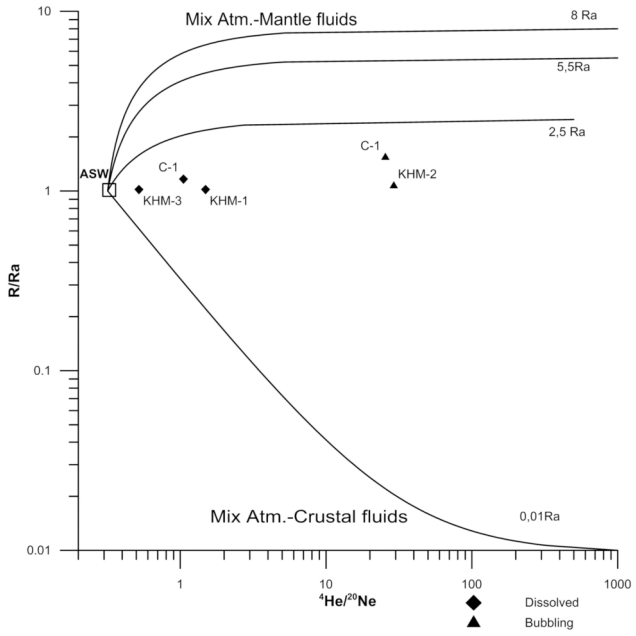

Fig. 4. Helium isotopic ratios (as R/Ra values) and He/Ne relationships. The theoretical lines represent binary mixing trends for mantle-originated, crustal and atmospheric helium. The end member value for He/Ne ratios are 0.318 (Air), 1000 (crust and mantle); for He-isotopic ratios are 1Ra (air) 0.02Ra (crust) and helium with three different mantle-signature: MORB = 8Ra; Contaminated Mantle = 5.5Ra and Contaminated/Degassed mantle = 2.5Ra.

humid condition having high deuterium excess) may cause such a shifting (Craig, 1961). Cold waters (10 and 11) and the thermal water (6) have the same origin as a result of a shallow circulation; whereas Kigihamzan, Meman, Gokoglan and Cerme springs (1, 2, 3, 4, 5, 7 and 8) show similar origin due to deep circulation (Fig. 2). The oxygen-18 and deuterium enrichment of Ilipinar thermal spring (9) can be associated with a high enthalpy reservoir. The stable isotope compositions of the cold waters fall on the Local Meteoric Water Line (LMWL). On the other hand, the deuterium enrichment can clearly be seen in thermal waters plotted above the EMWL (Fig. 2). The possible explanations for the clustering of thermal waters above the EMWL are either a result of the silicate hydration or H_2S exchange (Geyh, 2000). The offset of Ilipinar spring (9) on EMWL may also indicate an isotopic fractionation with water-vapor exchange. The deuterium excess values (Table 2), which were calculated using the equation ($d = \delta D - 8\delta^{18}O$) proposed by Dansgaard (1964), indicate low humidity conditions during primary vapor formation in the study region. On the other hand, especially due to the existence of gypsum in the region within the sedimentary deposits of a paleo-lake deposition environment in the area, Cerme (7 and 8) and Ilipinar (9) springs, the sulfate in gypsum ($CaSO_4\ 2H_2O$) loose its oxygen in a reductive environment, and this causes the occurrence of H_2S. The idea of the occurrence of H_2S in thermal waters (a rotten egg smell was felt during the sampling at Cerme and Ilipinar thermal springs) probably leads to an increase in deuterium values (Balderer, 1999). Another alternative explanation for the enrichment of hydrogen isotope values with a slight decrease in oxygen isotope values of samples may be due to the interaction with Pliocene clays at quite low temperatures (O'Neil and Kharaka, 1976; Graham, 1981). However, hydrocarbon content may also lead to change in hydrogen isotope composition for displacement of sample 14 (KHM3) with two order higher CH_4 content relative to sample 13 (KHM1). Furthermore, a relative strong CO_2 degassing in the sample 14 to the sample 13 (in consistent with their pH values) may also cause enrichment in oxygen-18 content of 14 which shifted to the right (Fig. 2). As to the sample 12, fractionation process besides gas water interactions probably modify isotopic composition as well as original gas composition.

Tritium values of Cerme waters (7 and 8) with 2.21–2.25 TU show a deep circulation while Yigitler thermal (6) and cold waters (10 and 11) can be considered as a rapid upward to the surface due to the high permeability along the fault zone which is consistent with higher tritium values, i.e., represents a shallow circulation (Fig. 3).

He and C isotopes

The collected samples have $^3He/^4He$ isotope ratios ranging from 1.03 to 1.54Ra_c for dissolved and bubbling gases, respectively. All the values are significantly above the crustal range of 0.02–0.05Ra (Andrews, 1985) and depict a probable mixture of crustal and mantle-type components.

The distribution of helium isotopic ratios versus the He/Ne ratios is shown in Fig. 4, where binary mixing curves display the trends drawn by mixtures of the atmosphere with different mantle and crustal sources. Conformingly, the presence of N_2 and O_2 in the sampled gases is clearly due to atmospheric contamination that occurred either because of intense bubbling (trapped air bubbles) and mixing of shallow air-saturated ground waters (ASW) with waters of deeper provenance. Although variable extents of atmospheric contamination are detectable in bubbling and dissolved gases, He content is always in concentrations well above the atmospheric, in agreement to the common feature that deep originated gases are CO_2-dominated and bring mantle and/or crustal-type helium. The samples from C1 and KHM2 fall close to mixing curve with atmospheric and mantle-derived helium. CO_2 content is almost above 80%, in both dissolved and bubbling gases.

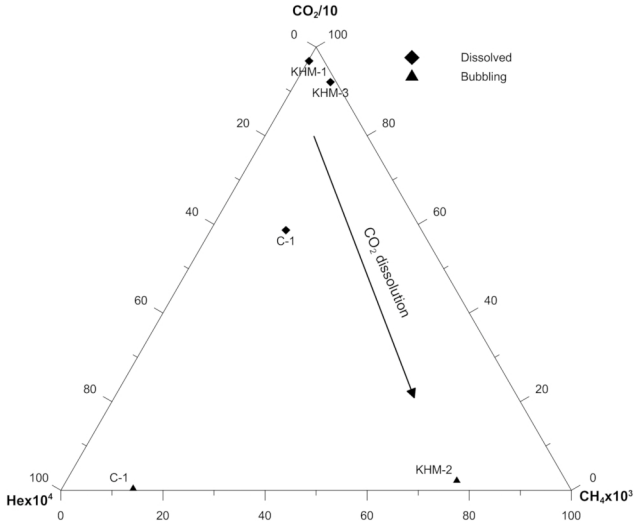

Fig. 5. CH_4–CO_2–He relationships for bubbling (filled black triangle) and dissolved gases (filled black diamond-shaped). The arrows show GWI effects with various extents of CO_2 dissolution.

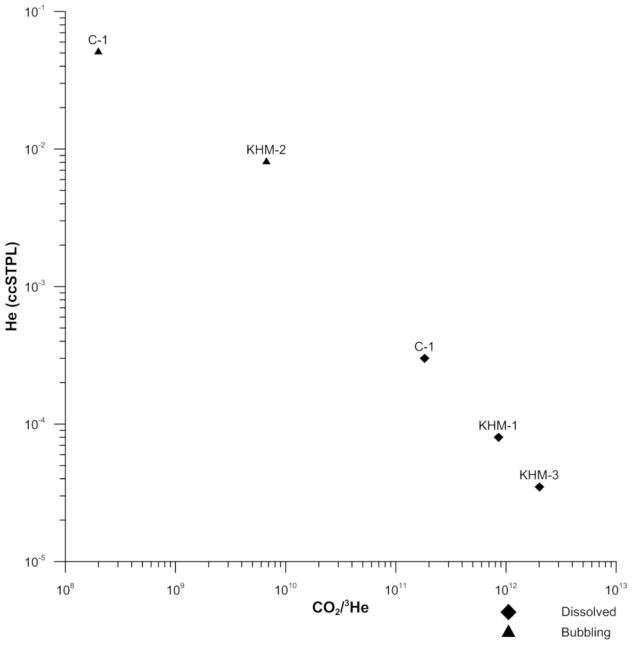

Fig. 6. $CO_2/^3He$ ratio versus He concentration. The arrow shows mantle derived contribution with increasing in the ratio of $CO_2/^3He$ and ^3He contents.

The CH_4–CO_2–He triangular diagram of Fig. 5 displays that CO_2 is relatively higher in dissolved than in bubbling gases. The arrow indicates trend for CO_2 loss due to GWI processes with the consequent enrichment of CH_4 in bubbles at KHM2. Besides GWI processes, calcite precipitation causes CO_2 loss as can be observed by the massive travertine deposits in the area. C1 mobility underwent enhanced GWI as shown by the low CO_2 concentration in the bubbling gases (24%) (Table 1). The reported analyses (Table 1) clearly show the absence of significant air contamination at KHM2. Contrastingly, large amounts of both O_2 and N_2 are detected at C1 (2.68% of O_2 and 73.14% N_2) besides relatively large amounts of He (5×10^{-2}%) and CH_4 (8.3×10^{-2}%). Although deep originated gases interact and probably equilibrate in deep aquifers before upraising to the surface, the evidence of the low CO_2 concentration (66 cm^3STP/L, far away from the CO_2 saturation in water of 762 cm^3STP/L; Weiss, 1971) besides the enhanced helium content (2.2×10^{-4} cm^3STP/L) in the dissolved gases at C1 site, leads us to expect the occurrence of repeated subsurface GWI processes responsible for CO_2 remove from the gas phase. He enriches in bubles at C1 while CO_2 degassing possible due to mantle-derived contribution.

Considering the higher CO_2 solubility in water compare to those of CO and CH_4, we could expect that both the CO_2/CO and CO_2/CH_4 ratios have been modified by gas-water interactions as suggested for some gas samples showing relatively low CO_2 contents (24 vol% at C1).

The various CO_2 sources, normally marked by different $\delta^{13}C$ ratios ($\delta^{13}C$ –6.5‰ in MORB; 0‰ limestones, –20‰ marine sediments; from –70 to –30‰ organic sources; Faure, 1986; Javoy *et al.*, 1986; Sano and Marty, 1995), may produce similar $\delta^{13}C$ values by admixtures of different sources. Moreover, because of its reactivity, CO_2 may suffer a wide spectrum of secondary processes (e.g., isotopic fractionation, isotopic equilibrium, chemical reactions etc.) that modify both the original CO_2 content and its large $\delta^{13}C$ variability due to isotopic signature. The $\delta^{13}C$ data listed in Table 1, show that the isotopic composition of the dissolved carbon varies from –0.2‰ (vs. VPDB) to +3.4‰ (KHM2 and KHM1).

The samples C1 and KHM2, taken from free-gas phase, are relatively higher than those of liquid phase (i.e., C1 and KHM1). Because, He increases in free-gas phase due to preferential release from the liquid phase (Ray *et al.*, 2009). As a result, C1 and KHM2 have slightly higher ^3He contents, which eventually causes decreasing $CO_2/^3He$ ratio (Fig. 6). The $CO_2/^3He$ ratio are eleveted in the samples C1, KHM1 and KHM3 due to either degassing He or increasing CO_2 by interaction with carbonate reservoir rocks. The high $CO_2/^3He$ values may also be related to hydrothermal degassing since He is less soluble in the aqueous phase compare to the gas-phase and this leads a relative increase in the $CO_2/^3He$ ratio in the dissolved samples (C1, KHM1 and KHM3). However, either dissolved or free-gas phase, $^3He/^4He$ isotope ratios of the samples are higher than crustal range (0.02).

Table 3. Estimated reservoir temperatures by using silica and cation geothermometers in the study area

Sample ID	1	2	3	4	5	6	7	8	9
T (°C)	56.9	56.3	35	34	53	51.6	34.9	34.4	29
Quartz	114.41	106.99	109.09	107.38	99.516	97.492	81.924	79.250	34.273
Chalcedony	85.492	77.457	79.727	77.879	69.419	67.252	50.711	47.892	14.657
Na–K–Ca–Mg	62.513	60.462	58.799	65.522	40.154	46	109.3	99.08	166.71
Na–Li	205.42	184.98	169.4	316.72	—	—			—

Quartz: $T = 1309/(5.19 - \log SiO_2) - 273.15$ *(Fournier, 1977).*
Chalcedony: $T = 1032/(4.69 - \log SiO_2) - 273.15$ *(Fournier, 1977).*
Na–K–Ca–Mg (meq/l) (Magnesium corrected): $R = (Mg/Mg+Ca+K) \times 100$ *(Fournier and Potter, 1979).*
Na–Li: $T = 1590/(0.779 + \log(Na/Li)) - 273.15$ *(Kharaka et al., 1982).*

Application of geothermometers

Geothermometers are used in the temperature estimation of fluids in the aquifers. The solubility of minerals is a function of temperature, pressure, and pH. Silica geothermometer can give more realistic results for the estimation of reservoir temperature if it varies between 120 and 180°C (Arnorsson and Gunnlaugsson, 1985). Chalcedony geothermometer can also be utilized if the temperature of geothermal system below 190°C (Henley *et al*., 1985; Fournier, 1977). Cation geothermometers are also widely used to estimate reservoir temperature. However, there are some limitations in the use of geothermometers (Karingithi, 2009). For example: Na–K geothermometer can not be used if the waters contain high concentration of Ca ion. As a result, Na–K geothermometer can only be applicable for the estimation of reservoir temperature of the water samples No. 7, 8 and 9. The estimated reservoir temperatures of water samples were given in Table 3.

If the equilibrium conditions do not exist, the values provided from geothermometers would not give reliable results. The existing negative values and some values even lower than the surface readings indicated that the water-rock equilibrium conditions have not been completely reached. As a conclusion, the results of geothermometers should be carefully taken into consideration. The validity of these geothermometers was taken under survey by many researchers. The Na–K–Mg triangular diagram has been developed by Giggenbach (1988) to estimate the temperature and to estimate whether the equilibrium has occurred between hot and mineralized waters and rocks in the aquifer. Giggenbach (1988) investigated the utilization of the triangular diagrams as chemical geothermometer for water samples according to the ion contents on the basis of the water-rock equilibrium. He classified the waters into three groups according to the Na, K and Mg ions. These are respectively: I) fully equilibrated waters; II) partially equilibrated waters; III) unbalanced waters. In waters within the first (I) zone, Na–K–Mg geothermometers may yield reliable results. For waters in the third (III) zone, where non-equilibrated waters exist (water-rock equilibrium does not occur); geothermometer applications could not reach sufficient results to determine the temperature of the aquifer (Tarcan, 2002). The appearance of the cold and thermal waters in Na–K–Mg triangular diagram is given in Fig. 7.

It can be seen from Fig. 7, the samples 7, 8 and 9 fall in partially equilibrated waters section (Zone II) and all other samples are located in the zone I where water-rock equilibrium does not exists (Zone I). Therefore, cation geothermometer gives erroneous results for these samples due to non-equilibrium condition in Zone I.

Mixing models

In many regions, when thermal waters are ascending to the surface, they mix with cold waters in certain ratios and reach to the surface with lower temperatures. This mixture also causes changes in the chemical composition of the original thermal water. As a result, the mineral equilibrium may be reached partially, totally or may not be reached. This situation may change according to the lithology of wall rock, the yield of the fluid, its temperature and its velocity towards the surface (Ongay, 2004). If the equilibrium takes place after the mixing; the results provided from the geothermometers do not indicate the temperature at depths but they give the temperature of the mixture. By using the alterations in chemical properties and temperature due to the mixing, several mixing models were developed to determine the temperature of the reservoir rock and mixing ratios. Fournier and Truesdell (1974) developed two models to estimate the temperature of the thermal water before the mixing: 1- First model is based on the silica content and temperature relation in thermal fluid, 2- Second model is constructed by temperature and chlorine content of thermal water. In this study, the mixing of thermal waters was investigated by using the first model.

The enthalpy/temperature-silica diagrams are a technique to estimate the temperature of thermal and mineralized waters by using temperature and silica equilibrium.

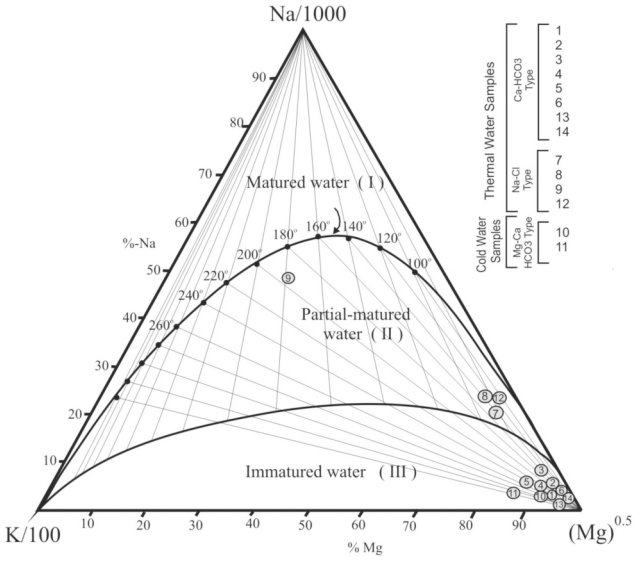

Fig. 7. The appearance of thermal and cold waters in Na–K–Mg triangular diagram and water-rock equilibrium temperatures (Giggenbach, 1988).

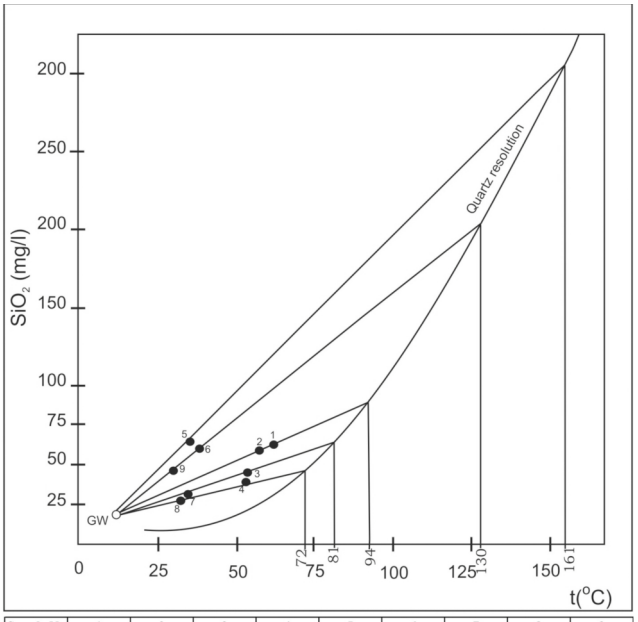

Sample No	1	2	3	4	5	6	7	8	9
Cold water mixing rate (%)	15	19	44	62.5	12.5	25	65	67.5	69

Fig. 8. Enthalpy-silica diagram of the study area with mixing ratios of thermal and cold waters (GW, Groundwater).

The success of the model is based on three basic assumptions: i) There is no any loss of temperature after the mixing, ii) The silica content of the fluid in the aquifer is controlled by the solubility of quartz, iii) After leaving from the aquifer and mixing with cold water, precipitation or dissolution of silica do not exist. The second assumption is always valid because of the saturation of the fluid to silica in depths. Due to the rapid precipitation of silica in high temperatures, the third assumption may not occur and may cause errors (Nicholson, 1993). In the enthalpy-silica mixing model, steam or temperature losses should not be taken place before mixing, and the aquifer temperature may be estimated under adiabatic cooling. When the silica-enthalpy diagram (Fig. 8) is taken into consideration, it is assumed that the aquifer temperature may range from 72 to 161°C. The silica-enthalpy diagram may also be used to estimate the mixing ratios of thermal and cold waters. The obtained results from this diagram are listed below Fig. 8, which shows that the dominant cold water mixing is observed in the thermal water sample No. 9 while the minimal mixing is seen in the samples No. 1 and 2.

CONCLUSIONS

An investigation was carried out to understand the geochemical features and origin of thermal fluids from Tekman (Erzurum) Geothermal Area. Water and bubbling gas samples have been collected from thermal waters with temperatures up to 57°C. Results indicate that geothermal waters associated with deep seated mantle-derived fluids and other deeply originated (magmatic) fluids move to the surface through fault/fracture systems.

Cerme and Ilipinar thermal springs (samples No. 7, 8, and 9) are classified as Na–Cl type water having deep circulation, while the other springs are of Ca–HCO_3 and Ca–Mg–HCO_3 type waters having relatively shallow circulation. Oxygen and hydrogen isotope results indicate that cold waters and Yigitler thermal water (6) have the similar origin through the shallow circulation, whereas Kigihamzan, Maman, Gokoglan, and Cerme thermal waters (1, 2, 3, 4, 5, 7, and 8) have the same origin characterized by the deeply circulated waters. In contrast to all other waters, the Ilipinar spring enriched in $\delta^{18}O$ thought to come from a source that has higher enthalpy. Cold waters are plotted on LMWL, while thermal waters are above the EMWL that can be affected by silicate hydration. On the basis of chemical composition and tritium values of the samples, Cerme thermal waters are assumed to come from a deep seated aquifer, while Yigitler (6) thermal water and cold waters (10 and 11) are of relatively from a shallow origin.

Based on the solute silica geothermometers, reservoir temperatures were calculated as 100–110°C for Gokoglan (4, 5) and Kigihamzan (1, 2) thermal springs. However, reservoir temperatures of 7, 8 and 9 springs were estimated as 100–160°C based on Na–K–Ca model.

According to the silica-enthalpy diagram, cold waters

are mixed at Cerme and Ilipinar springs (7, 8, and 9) and thus the waters cooled during ascending to the surface. $CO_2/^3He$ values and He contents at each sample location; CO_2 production followed by calcite precipitation and GWI processes leading to CO_2 dissolution are responsible for the chemical composition including the CO_2 contents and $\delta^{13}C$ values.

Gas geochemistry results also indicate that Kigihamzan and Catak samples (KHM1, KHM2, KHM3, and C1) represent deeply originated (magmatic) fluids mixing with crustal fluids under the fractionation by hydrothermal degassing. In light of all evaluations above, it can be concluded that heat source of the geothermal system is assumed as a magma chamber, where the Bingol Mountain lavas intruded. Furthermore, Upper Miocene Kohkale Tepe and Middle–Late Pliocene Yolustu Formation are the cap rocks. The reservoir rock is the jointed Adilcevaz Formation outcropping in the southern part of the area. When all these observations are evaluated, a possible high enthalpy geothermal reservoir appears possible from Gokoglan (3 and 4) to Cerme thermal springs (7 and 8). In fact, an exploitable geothermal fluid having a quite high yield at reasonable temperature was obtained from a well that was drilled in Cerme, close to the study area.

Acknowledgments—The study was funded by General Directorate of Mineral Research and Exploration (MTA) as a research project. The authors would like to thank Hayrullah Dagistan, Hanifi Gurler, Sinan Sarp, Nilgun Dogdu, Talat Yildirim and Ibrahim Yılmaz for their valuable contributions in the project. We extend our thanks to Technical Research and Quality Control Department of State Hydraulic Works (DSI) and MTA Laboratories for their supports. The authors would also like to thank Dr. Tonguc Uysal and anonymous reviewer/s for their helpful guidance in the development of the paper.

REFERENCES

Andrews, J. N. (1985) The isotopic composition of radiogenic He and its use to study groundwater movement in confined aquifer. *Chem. Geol.* **49**, 339–351.

Arnorsson, S. and Gunnlaugsson, E. (1985) New gas geothermometers for geothermal exploration—calibration and application. *Geochim. Cosmochim. Acta* **49**, 1307–1325.

Arpat, I. E. and Saroglu, F. (1975) Some important tectonically events in Turkey. *The Bulletin of Turkish Geological Society* **18/1**, 91–101 (in Turkish).

Balat, M. (2006) *Current Geothermal Energy Potential in Turkey and Use of Geothermal Energy Sources, Part B: Economics, Planning and Policy*. 65 pp.

Balderer, W. (1997) Mechanisms and processes of groundwater circulation in tectonically active areas. *Active Tectonics of Northwestern Anatolia—The Marmara Poly-Project* (Schindler, C. and Pfister, M., eds.), vdf Hochschulverlag AG an der ETH, Zurich, 415 pp.

Balderer, W. (1999) Application of isotope techniques in hydrogeology. Faculty of Mines Press, İstanbul Technical University, İstanbul, 356 pp.

Battocletti, L. (1999) Geothermal resource in Turkey. Report No. INEEL/EXT-99-01282, Bob Lawrence & Associates, 68 pp.

Bozkurt, E. (2001) Neotectonics of Turkey, A synthesis. *Geodinamica Acta* **14**, 3–30.

Can, A. R., Yildirim, N. and Ozbayrak, I. H. (1987) Erzurum-Ilica (E-1) sicaksu sondaji kuyu bitirme raporu. MTA report No. 8323, Mineral Research and Exploration Institute, Ankara, Turkey (in Turkish).

Canik, B. and Baskan, E. M. (1983) IAH map of mineral and thermal waters of Turkey Aegean Region. MTA report No. 189, Mineral Research and Exploration Institute, Ankara, Turkey.

Cetin, H., Güneyli, H. and Mayer, L. (2003) Paleoseismology of the Palu-Lake Hazar segment of the East Anatolian Fault Zone, Turkey. *Tectonophysics* **374**, 163–197.

Conrad, M. A., Hipfel, B. and Satır, M. (1995) Chemical and stable isotopic characteristics of thermal waters from Cesme-Seferihisar Area, Izmir (W. Turkey). *Int. Earth Science Coll. on the Aegean Region, 1995*, program and abstracts, 669.

Craig, H. (1961) Isotopic variations in meteoric waters. *Science* **133**, 1702–1703.

Dagistan, H., Dogu, N. and Karadaglar, M. (2010) Geothermal explorations and investigations by MTA in Turkey. *Poceedings World Geothermal Congress 2010*, Bali, Indonesia, 25–29 April 2010.

Dansgaard, W. (1964) Stable isotopes in precipitation. *Tellus* **16**, 436–468.

Demange, J., Gauthier, P. and Puvilland, P. (1989) Germencik geothermal field feasibility report. Part one geothermal model. 89 CFG 50, France.

Demirtasli, E. and Pisoni, C. (1965) Ahlat-Adilcevaz bolgesinin jeolojisi (Van golu kuzeyi). *Journal of MTA* **64**, 22–36 (in Turkish).

Ercan, T., Satir, M., Turkecan, A., Akyurek, B., Cevikbas, A., Gunay, E., Ates, M. and Can, B. (1985) Bati Anadolu Senozoyik volkanitlerine ait yeni kimyasal, izotopik ve radyometrik verilerin yorumu (Interpretation of new chemical, isotopic and radiometric data from the Cenozoic volcanics of western Anatolia). *Bulletin of the Geological Society of Turkey* **28**, 121–136.

Ercan, T., Satir, M., Sevin, D. and Turkecan, A. (1997) Some new radiometric ages from Tertiary to Quaternary volcanic rocks from W. Anatolia (Turkey). *MTA Dergisi* **119**, 103–112.

Eyidogan, H. (1988) Rates of crustal deformation in western Turkey as deduced from major earthquakes. *Tectonophys* **108**, 83–92.

Faure, G. (1986) *Principles of Isotope Geology*. 2nd edition, Wiley, New York, 589 pp.

Favara, R., Grassa, F., Inguaggiato, S., Pecoraino, G. and Capasso, G. (2002) A simple method to determine the $\delta^{13}C$ content of total dissolved inorganic carbon. *Geofísica Internacional* **41**, 313–320.

Fournier, R. O. (1977) A review of chemical and isotopic

geothermometers for geothermal systems. *Proceeding of the Symposium on Geothermal Energy, Cento Scientific Program*, 133–143.

Fournier, R. O. and Potter, R. W. (1979) Magnesium correction to the Na–K–Ca chemical geothermometer. *Geochim. Cosmochim. Acta* **43**, 1543–1550.

Fournier, R. O. and Truesdell, A. H. (1974) Geochemical indicators of subsurface temperature—part 2, Estimation of temperature and fraction of hot water mixed with cold water. *U.S. Geol. Surv. J. Res.* **2**(3), 263–270.

Gemici, U. and Filiz, S. (2001) Hydrochemistry of the Cesme geothermal area in western Turkey. *J. Volcanol. Geotherm. Res.* **110**, 171–187.

Geyh, M. (2000). Environmental isotopes in the hydrological cycle. *Principles and Applications* (Mook, W. G., ed.), Volume IV, Groundwater, saturated and unsaturated zone, IHP-V, *Technical Documents in Hydrology 1, No. 39, Vol. IV*, 196.

Giggenbach, W. F. (1988) Geothermal solute equilibria. Derivation of Na–K–Mg–Ca geoindicators. *Geochim. Cosmochim. Acta* **52**, 49–65.

Gokgoz, A. (1998) Geochemistry of the Kızıldere–Tekkehamam–Buldan–Pamukkale geothermal fields, Turkey. *Geothermal Training in Iceland 1998* (Georgsson, L. S., ed.), 115–156, United Nations University Geothermal Training Programme, Reykjavik, Iceland.

Graham, C. M. (1981) Experimental hydrogen studies III: Diffusion of hydrogen in hydrous minerals and stable isotope exchange in metamorphic rocks. *Contrib. Mineral. Petrol.* **76**, 216–228.

Gulec, N. (1988) The distribution of helium-3 in Western Turkey. *Mineral Res. Expl. Bull.* **108**, 35–42.

Gurer, A., Gürer, Ö. F., Pinçe, A. and Ilkisik, O. M. (2001) Conductivity structure along the Gediz Graben, West Anatolia, Turkey: Tectonic implications'. *Inter. Geol. Rev.* **43**(12), 1129–1144.

Henley, R. W., Truessdell, A. H., Barton, P. B. and Whitney, J. A. (1985) Fluid-mineral equilibria in hydrothermal systems. *Rev. Econ. Geol.* Vol. I, 267.

Hilton, D. R., Gronvold, K., Sveinbjornsdottir, A. E. and Hammerschmidt, K. (1998) Helium isotope evidence for off-axis degassing of the Icelandic hot spot. *Chem. Geol.* **149**, 173–187.

Hurbert-Ferrari, A., King, G., Van Der Woerd, J., Villa, I., Altunel, E. and Armijo, R. (2009) *Long-term evolution of the North Anatolian Fault; New constraints from its eastern termination*. 140 pp.

Imbach, T. (1997) Deep groundwater circulation in the tectonically active area of Bursa, Northwest Anatolia, Turkey. *Geothermics* **26**, 251–278.

International Organization for Standardization (ISO) (1989) Water quality-determination of tritium activity concentration—Liquid Scintillation Counting method international standard ISO 9698:1989(E). Geneva, Switzerland.

Italiano, F., Bonfanti, P., Ditta, M., Petrini, R. and Slejko, F. (2009) Helium and carbon isotopes in the dissolved gases of Friuli region (NE Italy): geochemical evidence of CO_2 production and degassing over a seismically active area. *Chem. Geol.* **266**, 76–85.

Italiano, F., Sasmaz, A., Yuce, G. and Okan, O. O. (2013) Thermal fluids along the East Anatolian Fault Zone (EAFZ): Geochemical features and relationships with the tectonic setting. *Chem. Geol.* **339**, 103–114.

Javoy, M., Pineau, F. and Delorme, H. (1986) Carbon and nitrogen isotopes in the mantle. *Chem. Geol.* **57**, 41–62.

Karingithi, C. W. (2009) *Chemical Geotermometers for Geothermal Exploration, Presented at Short Course IV on Exploration for Geothermal Resources*, organized by UNU-GTP, KenGen and GDC, Lake Naivasha, Kenya.

Keskin, M. (2007) Eastern Anatolia: a hotspot in a collision zone without a mantle plume. *Plates, Plumes, and Planetary Processes, Special Paper, Vol. 430* (Foulger, G. R. and Jurdy, D. M., eds.), 693–722, Geological Society of America.

Kharaka, Y. K., Lico, M. S. and Law-Leroy, L. M. (1982) Chemical geothermometers applied to formation waters, Gulf of Mexico and California basins. *Am. Assoc. Petrol. Geol. Bull.* **66**, 588–600.

Mertoglu, O., Bakir, N. and Kaya, T. (2003) Geothermal applications in Turkey. *Geothermics* **32**, 419–428.

Mutlu, H. and Gulec, N. (1998) Hydrogeochemical outline of thermal waters and geothermometry applications in Anatolia (Turkey). *J. Volcanol. Geotherm. Res.* **85**, 495–515.

Mützenberg, S. (1997) Nature and origin of the thermal springs in the Tuzla area, Western Anatolia, Turkey. *Active Tectonic of Northwestern Anatolia—The Marmara Poly-Project* (Schindler, C. and Pfister, M., eds.), 301–317, vdf hochschulverlag AG an der ETH, Zurich.

Nicholson, K. (1993) *Geothermal Fluids, Chemistry and Exploration Techniques* **22**, 13–33, Springer-Verlag, Heidelberg, Berlin.

Olmez, E. and Güner, A. (1989) Van-Ercis-Zilan gradyan sondaji (ZG-1) kuyu bitirme raporu. MTA report No. 8724, Mineral Research and Exploration Institute, Ankara, Turkey, 37 pp. (in Turkish).

O'Neil, J. R. and Kharaka, Y. K. (1976) Hydrogen and oxygen isotope exchange reactions between clay minerals and water. *Geochem. Cosmochim. Acta* **40**, 241–246.

Ongay, E. (2004) Hydrogeological and Hyrdochemical investigation of Balıkesir–Pamukçu Geothermal Area and its Vicinity. M.Sc. Thesis, Institute of Science, Dokuz Eylul University, 146 pp. (in Turkish).

Ozgur, N., Vogel, M., Pekdeğer, A., Halback, P. and Sakala, W. (1998) Geochemical, hydrochemical, and isotopic geochemical signatures of thermal fields in Kızıldere in the continental rift zone of the Buyuk Menderes, western Anatolia. *3rd International Turkish Geology Symp.*, Ankara, Turkey, **31**, 144.

Ozler, M. H. (2000) Hydrogeology and geochemistry in the Curuksu (Denizli) hydrothermal field, western Turkey. *Environ. Geol.* **39**, 1169–1180.

Ray, M. C., Hilton, D. R., Munoz, J., Fischer, T. P. and Shaw, A. M. (2009) The effects of volatile recycling, degassing and crustal contamination on the helium and carbon geochemistry of hydrothermal fluids from the Southern Volcanic Zone of Chile. *Chem. Geol.* **266**, 38–49.

Sano, Y. and Marty, B. (1995) Origin of carbon in fumarolic gas from island arc. *Chem. Geol.* **119**, 265–274.

Saroglu, F. (1986) Geologcial and tectonical evaluation of eastern Anatolia in neotectonic era. Ph.D. Thesis, Institute of Science, Istanbul University, 101 pp. (in Turkish).

Sayın, M. and Eyuboglu, O. S. (2005) Determination of the local meteoric water lines using stable isotope contents of precipitation in Turkey. *2nd National Symposium of Isotope Techniques in Hydrology* **323–344**, 26–30 (in Turkish).

Serpen, U., Aksoy, N. and Ongur, T. (2010) Present status of geothermal energy in Turkey proceedings. *Thirty-Fifth Workshop on Geothermal Reservoir Engineering Stanford University*, 188–198.

Simsek, S. (1982) Geology, geochemistry, and geothermal model of the Kizildere geothermal field. *First Turkish-Italian Seminar on Geothermal Energy*, Turkey, 1–25.

Simsek, S. (1997) Geothermal potential in northwestern Turkey. Active tectonics of northwestern Anatolia. *The Marmara Poly-Project* (Schindler, C. and Pfister, M., eds.), 111–123, vdf hochschulverlag AG an der ETH, Zurich.

Tarcan, G. (2002) Geothermal water chemistry, centre of geothermal energy. *Research and Application (Jenarum), Summer School Publications*, 87–113 (in Turkish).

Tarcan, G. and Gemici, U. (2003) Water geochemistry of the Seferihisar geothermal area, Izmir, Turkey. *J. Volcanol. Geotherm. Res.* **126**, 225–242.

Tarhan, N. (1991a) The geology and Petrology of Hınıs-Varto-Karlıova (Erzurum-Muş-Bingöl) Vicinity. MTA Report, No. 9428, 48 pp. (in Turkish).

Tarhan, N. (1991b) The geology and Petrology of Neogene Volcanites Around Hınıs-Varto-Karlıova (Erzurum-Muş-Bingöl). *MTA Journal* **113**, 45–60 (in Turkish).

Tarhan, N. (1997) 1:100,000 in scale Geological Map of Turkey, Erzurum-G 32 sheet. MTA Publications, Ankara, 31 pp.

Taskiran, L. (2006) Hydrogeochemical investigation of thermal spring waters in southwest of Tekman (Erzurum). M.Sc. Thesis, Eskisehir Osmangazi University, 61 pp. (in Turkish).

Vengosh, A. and Helvacı, C. (2002) Geochemical constraints for the origin of thermal waters from western Turkey. *Appl. Geochem.* **17**, 163–183.

Vengosh, A., Helvacı, C. and Karamanderesi, I. H. (2002) Geochemical constraints for the origin of thermal waters from western Turkey. *Appl. Geochem.* **17**, 163–183.

Weiss, R. F. (1971) Solubility of helium and neon in water and seawater. *J. Chem. Eng. Data* **16**, 235–241.

Yılmaz, Y. (1997) Geology of western Anatolia. *Active Tectonics of Northwestern Anatolia—The Marmara Poly-Project* (Schindler, C. and Pfister, M., eds.), 31–53, vdf Hochschulverlag AG an der ETH, Zurich.